

PHOTOMETRIC PROPERTIES OF THE OPEN CLUSTER NGC 2194

JAEMANN KYEONG¹, YONG-IK BYUN², AND EON-CHANG SUNG¹

¹Korea Astronomy & Space Science Institute, Taejeon 305-348, Korea

E-mail: jman@kasi.re.kr & ecsung@kasi.re.kr

²Department of Astronomy, Yonsei University, Seoul 120-749, Korea

E-mail: ybyun@yonsei.ac.kr

(Received October 5, 2005; Accepted November 7, 2005)

ABSTRACT

UBVIJHK photometry of the open cluster NGC 2194 are presented. Color-Magnitude diagrams of this cluster show well-defined main sequence and red giant clump. The main sequence also contains clear evidence of binary populations. Based on color-color diagrams, absolute magnitude of red giant clump, ZAMS fitting, and comparisons of observed color-magnitude diagrams with theoretical models, we derive following parameters for the cluster; reddening $E(B - V) = 0.44 \pm 0.04$, age of $\log t \sim 8.8$, and finally distance of $(m - M)_0 = 12.20 \pm 0.18$.

Key words : Hertzsprung — Russell(HR) diagram — Photometry — open cluster — NGC 2194

I. INTRODUCTION

The intermediate age open clusters present good opportunities to study the issue of convective overshooting (Barbaro & Pigatto 1984, Bertelli et al. 1985). They have turnoff masses near the critical value separating the region of core He-flash from that of He-ignition.

Recently, there are increasing number of attempts to characterize galactic open clusters. However we still suffer from the lack of homogeneous and consistent data for large number of open clusters, which make it difficult to investigate the formation and evolution scenario of galactic disk. In many cases, accurate estimate of dust reddening is also needed. We have therefore been carrying out a general near-infrared study for the Galactic clusters focusing on the intermediate age clusters and also making optical observations whenever necessary. We present here the outcome of our photometric study of the intermediate-age open cluster NGC 2194 [$\alpha_{1950} : 6^h 11^m$, $\delta_{1950} : 12^\circ 49'$], together with estimates of basic properties such as reddening, distance modulus, and age.

In §II the observation and data reduction process are described. In §III we discuss morphological features of the CMDs. In §IV we derive the basic parameters, reddening, distance modulus and estimates of the cluster age based on the prevailing methods. In §V, comparisons are made for the various CMDs with theoretical isochrones.

Corresponding Author: J. Kyung

II. OBSERVATION AND DATA CALIBRATION

(a) Optical Data

UBVI CCD photometry for the open cluster NGC 2194 was obtained during a five night observing program using the 40-inch telescope (f/8) and SITe 2048 \times 2048 CCD ($24\mu\text{m}$) at the Siding Spring Observatory starting from December 3, 1998. The plate scale is $0''.60/\text{pixel}$ and total field of view was $20'.5 \times 20'.5$. To correct for the intensity saturation and non-linearity range of bright stars, we obtained both long and short exposure frames for *B*, *V*, *I* filters. The detailed observing log is given in Table 1.

The data reduction procedure follows the standard CCD data operation using IRAF/CCDRED package. The images were flattened after overscan correction and bias/dark subtraction. Instrumental magnitudes were obtained using the pointing spread function (PSF) fitting packages of DAOPHOT II and ALLSTAR. Stars of different frames were matched by DAOMATCH /DAO-MASTER routines (Stetson 1992). For each frame, a number of unsaturated isolated stars are used to construct a good model PSF. Due to a slight optical distortion at the focal plane, it was necessary to allow the shape of model PSF to vary quadratically depending on positions in each frame. Finally, aperture corrections were made using the program DAOGROW (Stetson 1990) where correction terms were derived using the same stars used for the PSF construction.

In addition to object frames, 120 standard star measurements were made from eight Landolt standard star regions. Among them we excluded the stars of the following criteria; (a) saturated stars (b) stars with photometric measurement errors greater than 0.01mag (c) stars which were observed less than 5 times by Landolt (1992).

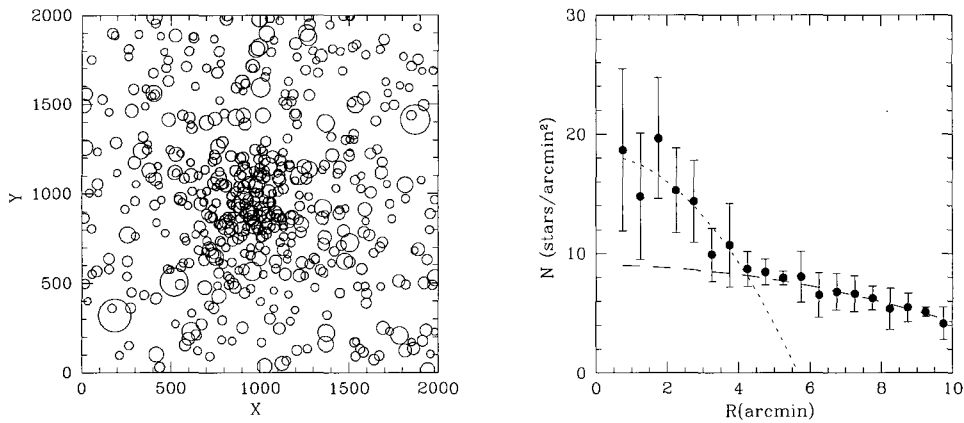


Fig. 1.— CCD observation field ($20' \times 20'$) (*left*). East is up, North is right. The X- and Y-axes are in pixels and 1 pixel corresponds to $0''.60$. Stars with $V < 16$ are marked to show the stellar distribution across the field. Projected surface number density profile (*right*) is constructed with stars of $V < 20$. Short dashed line represents major cluster concentration and long dashed line minor contribution (see text).

TABLE 1.
OBSERVING LOG

Obs Date	Filter	Short Exp (sec)	Long Exp (sec)	Airmass	FWHM(arcsec)
3 Dec. 1998	<i>U</i>		400	1.394	2.4
	<i>B</i>	100	400	1.438, 1.475	2.4
	<i>V</i>	50	200	1.584, 1.613	2.6
	<i>I</i>	30	100	1.510, 1.519	2.1
25 Dec. 1996	<i>J, H, K_n</i> [†]		1.0×20 cycles [‡]	1.504, 1.466, 1.437	1.3

^{†,‡} : see McGregor(1995) for details.

The transformation equations derived from standard star observations have following forms.

$$\begin{aligned}
 U &= u - [k_{1U} - 0.013(U - B)] X_U + C_U(U - B) + f(B - V)_0 + \zeta_U \\
 B &= b - [k_{1B} - 0.031(B - V)] X_B + C_B(B - V) + \zeta_B \\
 V &= v - k_{1V} X_V + C_V(B - V) + \zeta_V, \text{ or} \\
 &= v - k_{1V} X_V + C'_V(V - I) + \zeta'_V \\
 I &= i - k_{1I} X_I + C_I(V - I) + \zeta_I
 \end{aligned}$$

where lower case symbols represent instrumental magnitudes and the upper case symbols indicate standard magnitudes. X is airmass. Investigating the residual in the U filter, we found nonlinear term in bluer colors. The second order coefficient as well as the nonlinear term in U and B filter are adopted from Sung et al.(1998) while other coefficients are derived from our standard star observation. No other trends, such as UT term, were not found in the residuals. Finally adopted

transformation coefficients and errors are given in Table 2.

TABLE 2.
TRANSFORMATION COEFFICIENTS

Filter	k_1	C	ζ
<i>U</i>	0.510 ± 0.065	0.095 ± 0.020	-3.782 ± 0.012
<i>B</i>	0.280 ± 0.033	-0.095 ± 0.021	-1.705 ± 0.019
<i>V</i>	0.156 ± 0.025	0.072 ± 0.018	-1.553 ± 0.014
	0.156 ± 0.025	0.069 ± 0.026	-1.560 ± 0.022
<i>I</i>	0.050 ± 0.024	0.033 ± 0.009	-2.005 ± 0.022

We illustrate the observed CCD field ($20' \times 20'$) of this cluster in Fig. 1. In Fig. 1 (*left*), the size of the circle is proportional to the magnitude such that the brighter the star, the bigger the circle. It can be seen from this figure that this cluster is rich and that the center of cluster can be identified with ease. In practice,

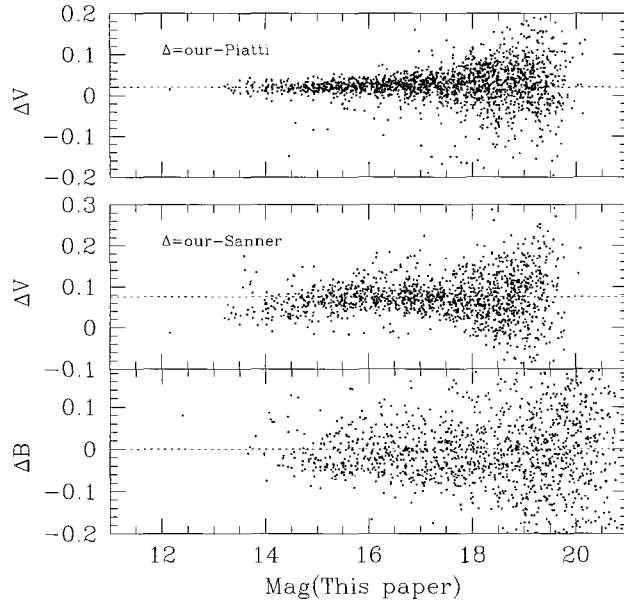


Fig. 2.— Comparison of our BV photometry of NGC 2194 with earlier studeis. The upper panel shows the comparison between this paper and Piatti et al. (2003) where the mean offset of dashed line is 0.02. The lower two panels show the comparisons between this paper and Sanner et al. (2000); these have poor agreements and the mean offset in V is 0.073 for $V > 18$.

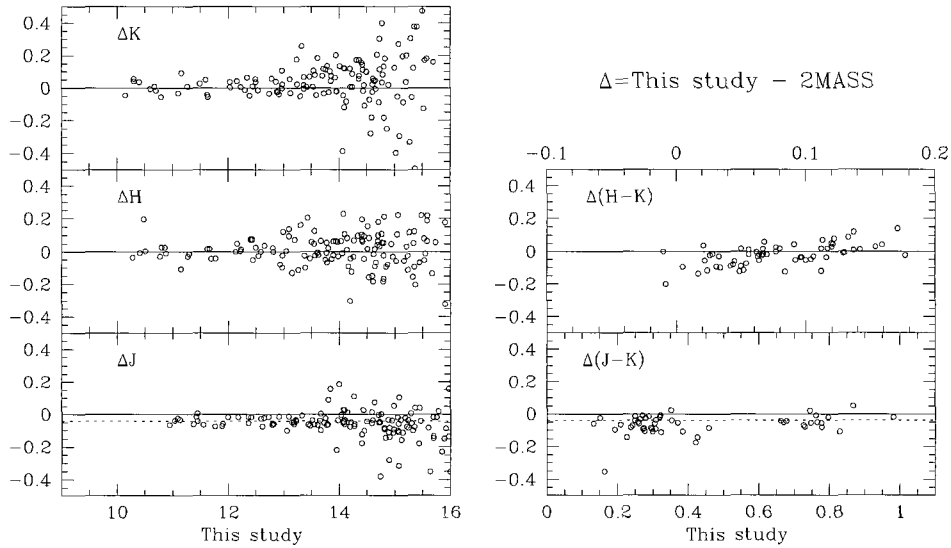


Fig. 3.— Comparison of our JHK photometry of NGC 2194 with the 2MASS data. The dashed lines in J and $J - K$ diagrams indicate an offset of 0.04 J-mag between ours and 2MASS data.

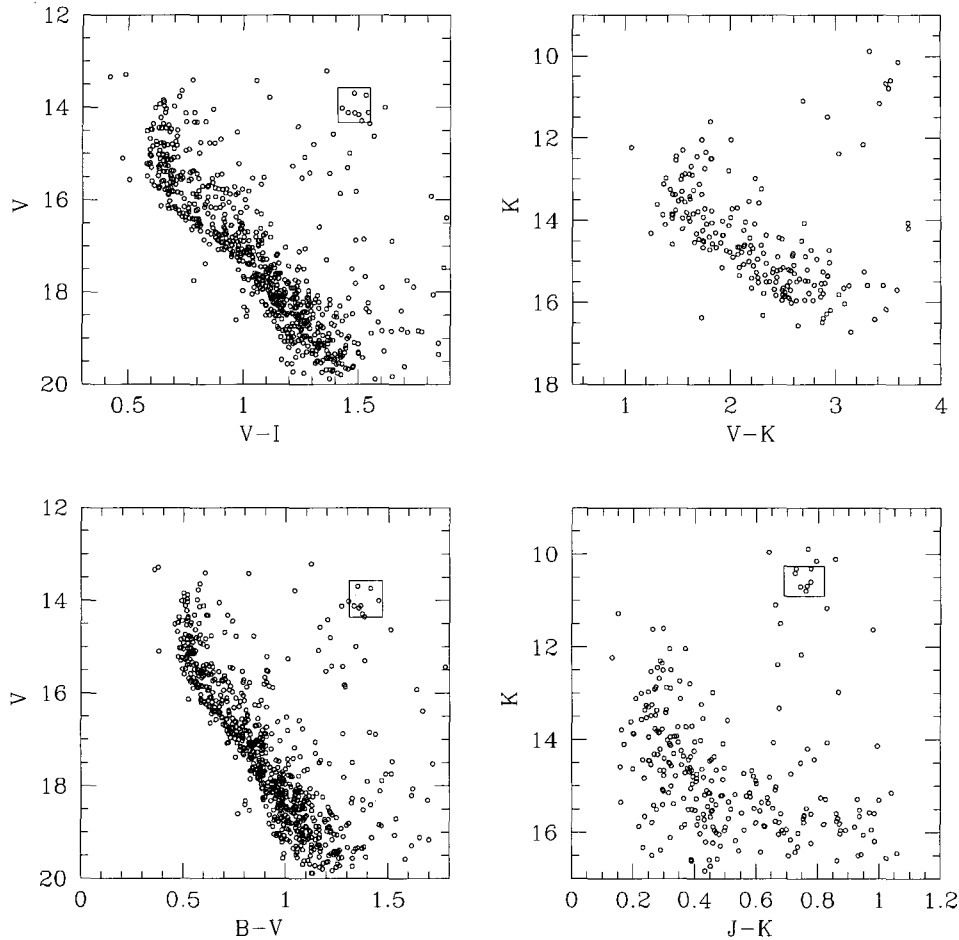


Fig. 4.— The optical and IR CMD of NGC 2194 using the stars inside $R < 4'$. The small box confine the red giant clump region.

the center of cluster is determined as the location which has the highest density from the star count. We have counted stars with the magnitude of $V < 20$ mag both to locate the exact cluster center and also to identify the radius range within which the contribution of the cluster stars are dominant. We fitted the polynomial along X- and Y-axis with 10 pixel bin and determined the central coordinates as $(X_C, Y_C) = (888, 902)$, which are converted to $(RA, DEC) = (6^h 13^m 47^s, 12^\circ 48' 11'', J2000)$.

Fig. 1 (*right*) display the projected radial profile of stellar number density of NGC 2194, again based on stars of $V < 20$. The number density profile shows two distinct components, strong concentration near the center and mild concentration outside. There seems to be a rather abrupt change in relative dominance of cluster stars at around the radius of $4.2'$. It is probable that there are some member stars beyond this radius, but we cannot discriminate the field interlopers and mem-

ber stars using photometric data only. The stars within this radius however are certainly dominated by cluster population, and therefore we use only these stars to investigate basic cluster properties.

There are two sets of published optical photometry of NGC 2194 by Sanner et al. (2000) and Piatti et al. (2003). We have compared their photometric data with our photometry in Fig. 2. In comparison with V photometry by Sanner et al. (2000), the mean offset is rather large being $\Delta V \sim 0.073$ ($V < 18$). In addition, some nonlinear trend is also apparent. This problem was previously noticed by Piatti et al. (2003), which indicates probable calibration problems in Sanner's data. In case of the comparison between ours and Piatti's, there is only a small mean offset of 0.02 mag in V . This difference can be regarded as negligible considering the transformation error of 0.036 mag in V .

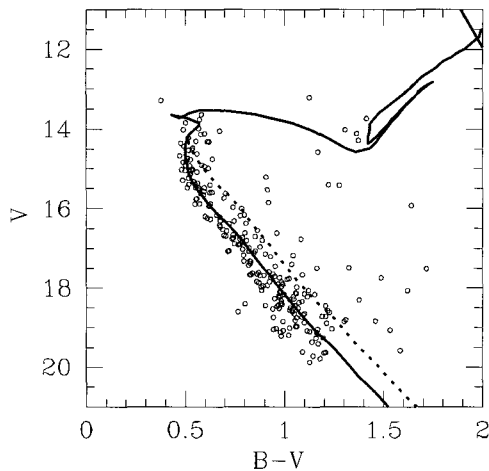


Fig. 5.— Equal mass binary sequence shown with the CMD of NGC 2194. The dashed line represents the 0.75 magnitude upward shift of the fitted isochrone ($\log t=8.8$, $[\text{Fe}/\text{H}]=-0.32$) following Bertelli et al. (1994). Only the central stars ($R < 2'$) are plotted so that the binary population can be better resolved.

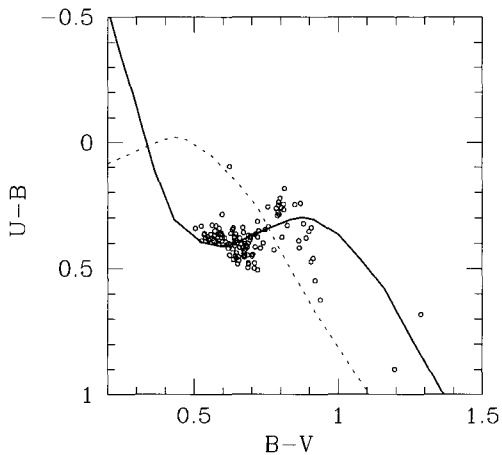


Fig. 6.— Color-color diagrams ($U - B, B - V$) of the central stars ($R < 4.2'$) constructed for the reddening determination. The dashed line represents the unreddened ZAMS line given by Sung & Bessell (1999) and the solid line is for $E(B - V)=0.44$. The open circles represent main sequence stars with observational error smaller than 0.03 mag.

(b) Near-Infrared Data

JHK images of the open cluster NGC 2194 were obtained over the night of December 25, 1996 using the 2.3m telescope and the IR camera CASPIR at the Siding Spring Observatory. CASPIR gives a gain of $9e^-/\text{ADU}$ and readout noise of 50 electrons. The detector of CASPIR was InSb chip of 256×256 format with the image scale of $0''.50/\text{pixel}$, which gave the sky coverage of $2.1 \times 2.1 \text{ arcmin}^2$. Since the field of view is very small, we did 2×2 mosaic observation to cover the wide field of NGC 2194. Each data frame was obtained with 1 second exposure time and 20 cycles, which means that each image is a combination of 20 frames of the same exposure time. Throughout the night, we frequently obtained bias frames because the bias level was known to vary at the time of observations (McGregor 1995). The detailed reduction method and the transformation equations of these IR data are given by Kyeong et al. (2004).

Carpenter et al. (2001) derived the relation between SAAO filter system (Carter 1990) adopted by us and the filter system used in 2MASS. We compared our *JHK* photometric results with 2MASS data in Fig. 3 after appropriate filter transformation. There are no systematic offsets in *H* and *K* magnitudes while in *J*-band we find about a small offset of 0.04 mag (weighted mean) for the stars brighter than $J \sim 14.0$.

III. COLOR MAGNITUDE DIAGRAM

Various color-magnitude diagrams (CMD) are shown in Fig. 4. A total of 2,832 stars are detected in optical band and 271 stars in near-IR band. But we plot only stars inside the major contribution radius of member stars ($\sim 4.2'$) in optical band and all stars in IR band. The overall CMD morphology resembles the CMD of typical intermediate age open cluster, for example, NGC 2477 (Kassis et al. 1997) and NGC 2660 (Sandrelli et al. 1999). There seem substantial field in-

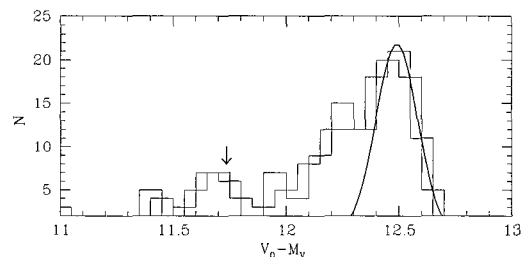


Fig. 7.— Distribution of distance moduli of NGC 2194 with a bin size of 0.1 mag in the ($V, B - V$) CMD, histogram extracted in overlaps to provide better resolution. In order to avoid the evolved star effect, only stars between $V=16-18$ mag were used. The downward arrow at ($V_0 - M_V \sim 11.75$) indicate the location of equal mass binary population.

terlopers because this cluster is located in the Galactic plane.

The broad main sequence in $(V, B - V)$ plane is quite clear due to the binaries. The general stellar locations are within the equal mass binary sequence. In Fig. 5, the stellar binary sequence is compared with the main-sequence isochrone shifted upward by 0.75 magnitude. Fig. 7 also shows a small but distinct presence of second peak near $V_0 - M_V \sim 11.75$ which contains the binary population.

We also measure the position of red giant clump (RGC) stars at $V=13.91$, $K=10.51$, $B - V=1.39$, $V - I=1.48$, $J - K=0.76$. Mean magnitudes of RGC will be used to refine the distance to the cluster (see Sec. IV(b)).

IV. CLUSTER PARAMETERS

(a) Reddening

The preferred method to determine the cluster reddening is to de-redden the $(U - B, B - V)$ colors using the reddening vector of $E_{U-B}/E_{B-V} = 0.72$.

To derive the reddening value we fit our data with the corrected ZAMS color-color curve with solar metallicity (Sung & Bessell 1999). In Fig. 6 we used only those main sequence stars of error less than 0.03 and within $R \sim 4.2'$. In case of $E(V - I)$, we adopted the relationship ($E(V - I) = 1.25E(B - V)$) as given by Dean et al. (1978). The error for each parameter is from the rms fitting error of the data within 1σ . Since NGC 2194 is located to the Galactic plane, it can be expected that the reddening is very significant. We obtained $E(B - V) = 0.44 \pm 0.04$. It is difficult to derive the reddening value in near-IR two-color diagram because the reddening line is parallel to reddening vector.

(b) Distance Modulus

Adopting the reddening value derived above, the distance to NGC 2194 can be estimated from main sequence fitting to the observed $(V, B - V)$ CMD. We obtained the apparent distance modulus of this cluster to be $(V_0 - M_V)_0 = 12.49 \pm 0.13$ from the ZAMS fitting. To increase the sample size and to reduce the binning effect we derived an additional overlapping distribution shifted by 0.05 mag. The 0.05 mag is negligible to fitting error of 0.13. In order to avoid the evolution effect, only stars between $V=16 \sim 18$ and $R < 4.2'$ were used.

The distance modulus derived by this method may suffer from metallicity effect, which affects stellar absolute magnitudes. Sung et al. (2002) derived $\Delta M_V = -0.90 [\text{Fe}/\text{H}]$ from the isochrones of Girardi et al. (2000). This relation produce the correction value of -0.24 mag when we adopt $[\text{Fe}/\text{H}] = -0.27$ for this cluster (Piatti et al. 2003). Final corrected distance modulus is therefore the $V_0 - M_V = 12.25 \pm 0.13$.

As the second method of distance determination, we considered the K -band absolute mean magnitude of

the red giant clump stars (RGC). The locations of RGC in different CMDs are shown in Fig. 4. In optical bands, the use of RGC as distance indicator is highly controversial (Sarajedini 1999, Cole 1998). But in K magnitude, the population effect (metallicity and age) is considered not significant (Grocholski & Sarajedini 2002, Alves 2000) and these studies show that the luminosity function of red giant clump peaks at $M_{K0} = 1.61 \pm 0.03$ mag using 2MASS and Hipparcos data analysis. The mean RGC K magnitude of NGC 2194 is measured at 10.51 ± 0.18 . From this value we obtained the distance as 12.1 ± 0.18 . Our estimates of the distance using above two methods are mutually consistent, and the average is $(m - M)_0 = 12.20 \pm 0.18$.

Janes & Phelps (1994) determined $E(B - V) = 0.51$ and $(m - M)_V = 13.75$ for NGC 2194. Sanner et al. (2000) derived $E(B - V) = 0.45$, $(m - M)_0 = 12.3$ from the optical data using isochrone fitting. Our $E(B - V)$ is slightly lower than Janes & Phelps (1994)'s value and in good agreement with Sanner et al. (2000)'s value.

(c) Age

Piatti et al. (2003) derived the metallicity of NGC 2194 from the Washington photometry as $[\text{Fe}/\text{H}] = -0.27$. Adopting this value we compared a set of isochrones against a C-M diagram of the cluster to establish the possible age range of the cluster. Isochrones were shifted to match the turnoff and the upper main sequence line in the cluster CMDs. Acceptability was based on how well the isochrones described the turnoff region, the slope and length of lower main sequence, location of the red giant clump. But RGC region was less emphasized in the comparison considering possible anomaly as pointed out by Mermilliod et al. (1998).

By comparing the theoretical model developed by Bertelli et al. (1994) to our observed C-M diagrams, we estimate the age of NGC 2194 as $\log t \sim 8.8$. The age range of $\log t = 8.7$ to 8.9 were tested, but most isochrones were eliminated as possible candidates because they poorly described the turnoff region and the slope of the main sequence. Isochrone fitting is shown in Fig. 8. Our value from this method are compatible with Sanner et al. (2000)'s estimate of $\log t = 8.74$.

V. ISOCHRONE FITTING AND SUMMARY

The best fitting isochrones plotted against the observed CMDs of NGC 2194 are shown in Fig. 9. The model fit comparison to NGC 2194 has $E(B - V) = 0.44$, $(m - M)_0 = 12.20$ and $\log t = 8.8$ with adopted Piatti et al. (2003)'s metallicity of $[\text{Fe}/\text{H}] = -0.27$. The isochrone fit for $(V, V - I)$ plane is noticeably worse than that for the $(V, B - V)$ plane. This mismatch in $(V, V - I)$ CMD appears to originate from the larger internal error of I magnitudes rather than from systematic error in determination of $E(V - I)$. Major discrepancies are most notable for $(K, V - K)$ plane, where most stars reside redder side of the theoretical

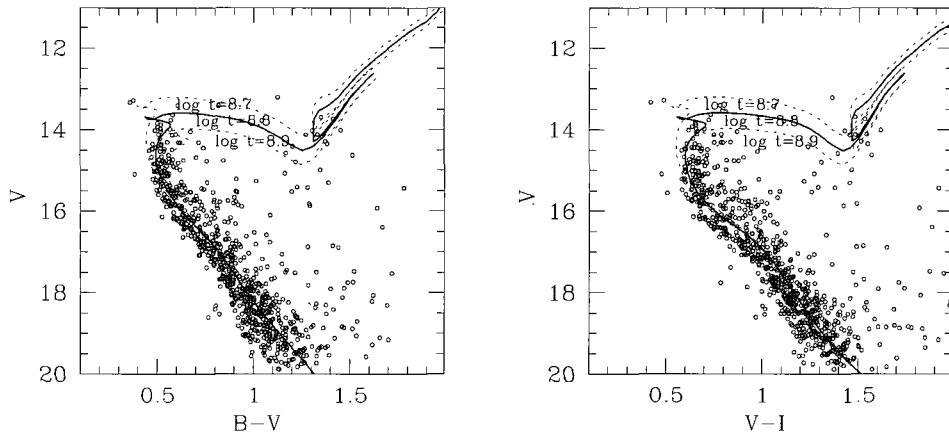


Fig. 8.— A grid of isochrones with $E(B - V)=0.44\pm 0.04$ and $(m - M)_0=12.20\pm 0.18$ are compared to NGC 2194 in a $(V, B - V)$ CMD. Stars inside $R < 4.2'$ are presented.

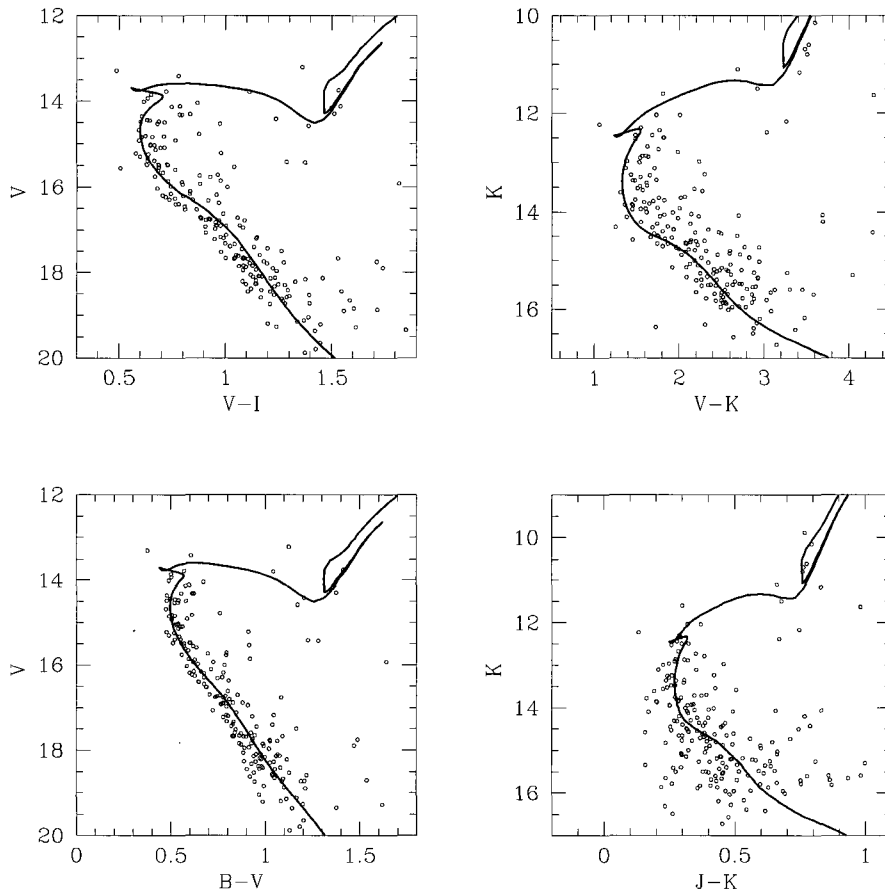


Fig. 9.— The isochrone with $\log t = 8.8$, $E(B - V)=0.44$, $(m - M)_0=12.20$ superimposed to the optical and IR CMDs. Only the stars detected in both optical and IR band are plotted.

predictions. We find no plausible explanation for this tendency.

The primary goal of this study is to present the optical and near-IR photometric data for stars in the field of NGC 2194 and also to derive physical parameters of the cluster. We derived following basic parameters; reddening $E(B - V) = 0.44 \pm 0.03$, distance modulus $(m - M)_0 = 12.20 \pm 0.18$ and constrained age of log $t \sim 8.8$ using a grid of model isochrones.

The thick appearance of the main sequence, at even small cluster radius ($R \sim 2'$), strongly suggests the existence of binary population rather than differential reddening. This is further supported by the fact that most of stars are located within the equal mass binary sequence upper boundary of 0.75 magnitude above the main sequence.

ACKNOWLEDGEMENTS

We would like to thank to the staffs of MSSSO of Australian National University to use their facilities. YIB acknowledges the support of Korea Research Foundation Grant (KRF-2002-070-C00045).

REFERENCES

- Alves, D. R., 2000, K-Band Calibration of the Red Clump Luminosity, *ApJ*, 539, 732
- Barbaro, G. & Pigatto, L., 1984, Red Giants in Old Open Clusters - A Test for Stellar Evolution, *A&A*, 136, 355
- Bertelli, G., Bressan, A., & Chiosi, C., 1985, Evolution of Intermediate Mass Stars - The Role of Convective Overshooting and Stellar Wind, *A&A*, 150, 33
- Bertelli, G., Bressan, A., Chiosi, C., Fagotto, F., & Nasi, F., 1994, Theoretical Isochrones from Models with New Radiative Opacities, *A&A* 106, 275
- Carpenter, J. M., 2001, Color Transformations for the 2MASS Second Incremental Data Release, *AJ*, 121, 2851
- Carter, B. S., 1990, Southern JHKL Standards, *MNRAS*, 242, 1
- Cole, A., 1998, Age, Metallicity, and the Distance to the Magellanic Clouds from Red Clump Stars, *ApJ*, 500, L137
- Dean, J. F., Warren, P. R., & Cousins, A. W., 1978, Reddenings of Cepheids using BVI photometry, *MNRAS*, 183, 569
- Girardi, L., Bressan, A., Bertelli, G., & Chiosi, C., Low-mass Stars Evolutionary tracks & isochrones, 2000, *A&AS*, 141, 371
- Grocholski, A. J. & Sarajedini, A., 2002, WIYN Open Cluster Study. X. The K-Band Magnitude of the Red Clump as a Distance Indica, *AJ*, 123, 1063
- Janes, K. A., Phelps, R. L., & Janes, K. A., 1994, The Galactic System of Old Star Clusters: The Development of the Galactic Disk. *AJ*. 108. 1773
- Kassisi, M., Janes, K. A., Friel, E. D., & Phelps, R. L., 1997, Deep CCD Photometry of Old Open Clusters, *AJ*, 113, 1723
- Kyeong, J. M., Byun, Y. I., & Sung, E. C., 2004, UBVI-JHK Photometric Study of the Open Cluster NGC 2849, *AJ*, 128, 2331
- Landolt, A. V., 1992, UBVR photometric Standard Stars in the Magnitude Range 11.5-16.0 around the Celestial Equator, *AJ*, 104, 340
- Mermilliod, J.-C., Mathieu, R. D., Latham, D. W., & Mayor, M., 1998, Red Giants in open Clusters. VIII. NGC 752, *A&A*, 339, 423
- McGregor, P., 1995, Users Manual for the CASPIR on the MSSSO 2.3m Telescope
- Piatti, A., Claria, J. J., & Ahumada, A. V., 2003, The Relatively Young and Metal-poor Galactic Open Cluster NGC 2194, *MNRAS*, 340, 1249
- Sandrelli, S., Bragaglia, A., Tosi, M., & Marconi, G., 1999, The Intermediate Age Open Cluster NGC 2660, *MNRAS*, 309, 739
- Sanner, J., Altmann, M., Brunzendorf, J., & Geffert, M., 2000, Photometric and Kinematic Studies of Open Star Clusters. II. NGC 1960 (M 36) and NGC 2194, *A&A*, 357, 471
- Sarajedini, A., 1999, WIYN Open Cluster Study. III. The Observed Variation of the Red Clump Luminosity and Color with Metallicity and Age, *AJ*, 118, 2321
- Stetson, P. B., 1990, On the Growth-Curve Method for Calibrating Stellar Photometry with CCDs, *PASP*, 102, 932
- Stetson, P. B., 1992, IAU Colloq. 136, Stellar Photometry, Current Techniques and Future Development, eds C. J. Butler & I. Elliot (Cambridge Press:Cambridge), 291
- Sung, H. & Bessell, M. S., 1999, UBVI CCD Photometry of M35 (NGC 2168), *MNRAS*, 306, 361
- Sung, H., Bessell, M. S., & Lee, S.-W., 1998, UBVR and H-alpha Photometry of the Young Open Cluster NGC 6231, *AJ*, 115, 734
- Sung, H., Bessell, M. S., & Lee, S.-G., 2002, The Open Cluster NGC 2516. I. Optical Photometry, *AJ*, 123, 290